

Magnetic transitions in $\text{CaMn}_7\text{O}_{12}$: a Raman observation of spin-phonon couplings

C. Toulouse^{1,2,*}, C. Martin³, M-A. Measson^{1,4,†}, Y. Gallais¹, A. Sacuto¹, and M. Cazayous¹
¹Laboratoire Matériaux et Phénomènes Quantiques (UMR 7162 CNRS), 75205 Paris Cedex 13, France
²Luxembourg Institute of Science and Technology, L-4422 Belvaux, Luxembourg
³Laboratoire de Cristallographie et Science des Matériaux (CRISMAT (UMR 6508)), 14000 Caen, France
⁴Institut Néel, CNRS/UGA UPR2940, 25 rue des Martyrs BP 166, 38042 Grenoble cedex 9
(Dated: June 30, 2021)

The quadruple perovskite Calcium manganite ($\text{CaMn}_7\text{O}_{12}$) is a multiferroic material in which a giant magnetically-induced ferroelectric polarization has been reported, making it potentially very interesting for magnetoelectric applications. Here, we report the Raman spectroscopy study on this compound of both the phonon modes and the low energy excitations from 4 K to room temperature. A detailed study of the Raman active phonon excitations shows that three phonon modes evidence a spin-phonon coupling at $T_{N2} \simeq 50$ K. In particular, we show that the mode at 432 cm^{-1} associated to Mn(B)O_6 (B position of the perovskite) rotations around the $[111]$ cubic diagonal is impacted by the magnetic transition at 50 K and its coupling to the new modulation of the Mn spin in the (a,b) plane. At low energies, two large low energy excitations are observed at 25 and 47 cm^{-1} . The first one disappears at 50 K and the second one at 90 K. We have associated these excitations to electro-magneto-active modes.

I. INTRODUCTION

Since the discovery of multiferroic materials, compounds combining a huge ferroelectric polarization and an important magnetoelectric coupling have been the goal for research in material synthesis.¹⁻³ Magnetoelectric multiferroic materials, combining ferroelectric and magnetic order in the same phase, can be classified in two categories⁴: type I materials in which the two orders appear independently at different transition temperature, exhibiting in general a low coupling between the two orders⁵, and type II materials where the ferroelectricity is induced by an another order (magnetic, orbital,

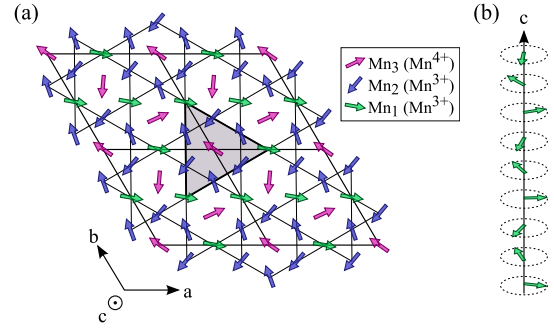


FIG. 2: Antiferromagnetic structure of $\text{CaMn}_7\text{O}_{12}$ appearing below 90 K (AFM_I phase). The spin of the Mn ions order antiferromagnetically in the (a,b) planes with superimposed long range spin spirals along the c axis.

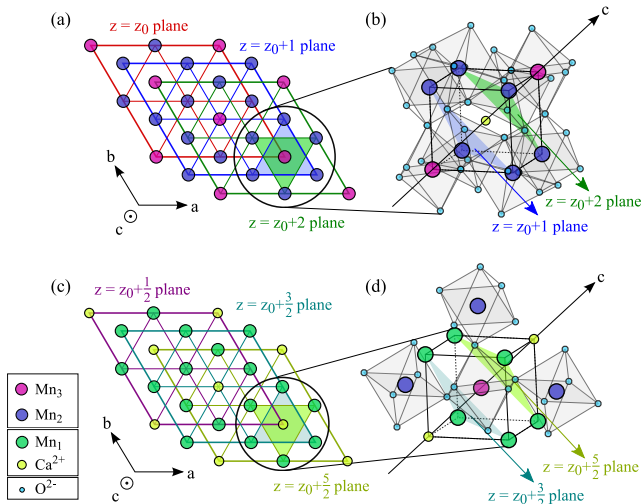


FIG. 1: Crystalline structure of $\text{CaMn}_7\text{O}_{12}$ shown in its trigonal ($R\bar{3}$ structure below 440 K. The different valence states (respectively Mn^{3+} and Mn^{4+}) of the Mn_2 and Mn_3 sites are responsible for the appearance of an additional orbital ordering under 250 K.

electronic)^{6,7}. The latter generally exhibit a much more important magnetoelectric coupling but have a small ferroelectric polarization ($\sim 100 \mu\text{C}\cdot\text{m}^{-2}$) appearing at very low temperature (below 30 K).

The exception is the quadruple calcium manganite, $\text{CaMn}_7\text{O}_{12}$, which has been synthesized as monocrystal of good quality only recently, which exhibits giant spin-induced polarization of $2870 \mu\text{C}\cdot\text{m}^{-2}$ in cycloidal AFM phase below 90 K.

Although this observation is supported by both experimental^{10,11} and theoretical^{12,13} works, the giant ferroelectricity in $\text{CaMn}_7\text{O}_{12}$ is currently under discussion. The high values of the polarizations reported in literature have been recently associated to extrinsic thermal effect rather to an intrinsic ferroelectricity¹⁴ although a very small ferroelectric polarization of $0.2 \mu\text{C}\cdot\text{m}^{-2}$ is still reported to subsist under 46 K.

Under 440 K, $\text{CaMn}_7\text{O}_{12}$ crystallizes in the trigonal $R\bar{3}$ space group¹⁵. Its structure is a quadruple ABO_3 rhombohedrally distorted perovskite structure with Ca and Mn ions (Mn_1 sites) sitting in the A sites and Mn ions

(Mn₂ and Mn₃ sites sitting in the B sites of the structure (see Fig. 1). This structural transition is accompanied by metal-insulator transition and charge ordering. The B-site Mn ions order into Mn₃⁺ and Mn₄⁺ with a 3 : 1 ratio.¹⁶ The subsequent structural helicoidal modulation of the Mn-Mn bond angles is incommensurate and propagates along $q_C \simeq (0, 0, 2.077)$.¹²

The manganese being a magnetic specie, the Mn³⁺ ($3d^4$, $S = 2$, $L = 2$) and Mn⁴⁺ ($3d^3$, $S = \frac{3}{2}$, $L = 3$) are responsible for the appearance of two successive magnetic orderings¹⁷. At $T_{N1} = 90$ K, the Mn spins orient in the (a, b) planes as shown in Fig. 2 and are coupled antiferromagnetically between neighboring planes (with 124° angles), forming incommensurate magnetic spirals along the 3-fold c axis. These spirals are coupled to the orbital ordering : they lie along the same direction with twice the wavelength of the orbital spirals. The propagation wavevector of the spin spiral is equal to $q_M = (0, 0, 1.037)$ ¹² in hexagonal notations or $k_1 = (0, 1, 0.963)$ in pseudo-cubic system¹¹. For the rest of the article, we will denote this phase AFM_I. Below $T_{N2} \simeq 50$ K, a second magnetic transition towards the AFM_{II} phase occurs and a new modulation of the Mn spins in the (a, b) planes appears corresponding to a ‘beating’ of the previous AFM_I order. The propagation wavevector of the spin spiral gives rise to two near propagation wave-vectors $k_{\pm} = k_1 \pm (0, 0, \delta)$.

The possible coupling between these magnetic orderings and a strong electric polarization arises questions regarding the mechanisms at stake in this compound. Moreover, it has been shown that the lattice degrees of freedom are actively involved in the orbital-ordering and magnetic mechanism.^{18,19} The study of the phonon modes and of the low energy excitations at the magnetic transitions by Raman spectroscopy is an efficient way to investigate the possible couplings between the different multiferroic orders. Up to now, very few Raman experiments have been reported^{18,20,22} on CaMn₇O₁₂. We present here a Raman investigation on both the low energy magnetic excitations and the phonon modes, with a focus on the temperature dependencies around the two magnetic transitions. At low temperature, it has been shown in powdered samples that the magnetostriction plays a role in the second magnetic transition at 50 K, and hence could be linked to our observations²². We have observed two additional excitations at low energies and could link them to the two magnetic transitions with their temperature behaviour. These two excitations have been identified as the Raman signature of CaMn₇O₁₂'s electromagnons.

II. EXPERIMENTAL DETAILS

The CaMn₇O₁₂ samples studied here are high quality single crystals of approximately $60 \times 60 \times 60 \mu\text{m}$ size. They have been grown by flux starting from a (CaCl₂:MnO₂) mixture with weight ratio (1:3) heated

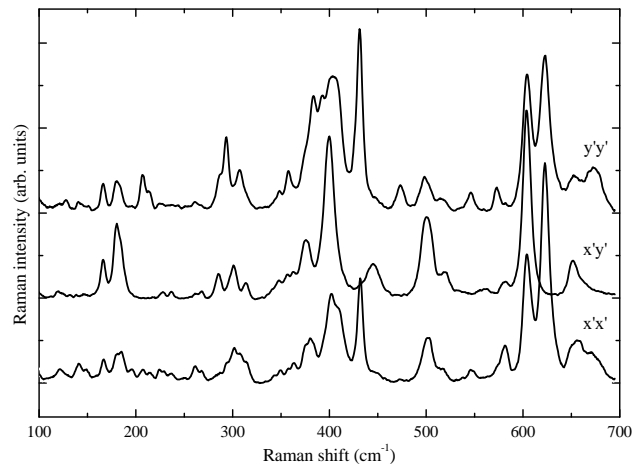


FIG. 3: Low temperature (10K) Raman spectra of phonon modes using cross-polarization ($x'y'$) and with parallel-polarization ($x'x'$ and $y'y'$) configurations. The associated assignments are derived from 20.

at 850°C for 24 hours and then cooled down at a rate of 5°C per hour. Bulk properties measurements and X-ray diffraction have been performed^{11,23} and showed no twinning at room temperature.

The Raman spectroscopy measurements were recorded using a triple subtractive T-64000 Jobin-Yvon spectrometer with a cooled CCD detector. The spectra were acquired using a 561.3 nm laser line from an Oxixus-Slim solid state laser, filtered both spatially and in frequency. Measurements between 10 and 300 K with an error bar of $\pm 2\text{K}$ have been performed using an ARS closed-cycle He cryostat. The instrumental response is a Gaussian with a FWHM of about 0.5 cm^{-1} . The conditions of sample preparation are important and only raw samples present a small background allowing to observe the low energy excitations.

III. RESULTS AND DISCUSSION

A. Lattice modes

CaMn₇O₁₂ crystallizes in the $R\bar{3}$ trigonal space group (148) and the total number of phonon modes at the Γ point is $\Gamma_{\text{TOT}} = 6A_g + 6E_g + 14A_u + 14E_u$. Twelve Raman active phonon modes are expected for first order processes at the Brillouin zone center : $\Gamma_{\text{Raman}} = 6A_g + 6E_g$.²⁰ Using different scattering configurations, it's possible to choose the mode to activate. Here we used incident wave vector anti-parallel to the scattered one (backscattering configuration). The E_g and $E_g + A_g$ modes are activated with cross-polarizations ($x'y'$) and with parallel-polarizations ($x'x'$ and $y'y'$), respectively. The x' and y' notations correspond to the directions parallel to the $[110]$ and $[\bar{1}10]$ quasicubic directions, respec-

tively.

TABLE I: Phonon modes measured by Raman spectroscopy compared with the modes measured in ref. 20. Note that the structure modulation below 250 K and in addition the breaking of space symmetry in the magnetic phase (IR modes become also Raman active) allow a higher number of modes.

Our work	Iliev & al.	
Energy (cm^{-1})	Energy (cm^{-1})	Mode assignment
78	–	–
99	–	–
122	–	–
140	–	–
150	–	–
168	167	E _g
180	179/180	E _g
186	185	A _g
207	207	A _g
215	211/215	A _g
227	–	–
238	–	–
262	–	–
269	–	–
287	285/286	E _g
294	–	–
301	301	E _g
309	306	E _g
316	314	E _g
352	–	–
359	–	–
364	–	–
375	376	E _g
380	–	–
385	390	E _g
403	400	E _g
410	412	A _g
432	428/432	A _g
452	–	–
472	473/474	A _g
493	497	E _g
501	501	E _g
518	–	–
533	–	–
546	–	–
560	–	–
580	597	E _g
605	604	E _g
622	623	A _g
652	651	E _g

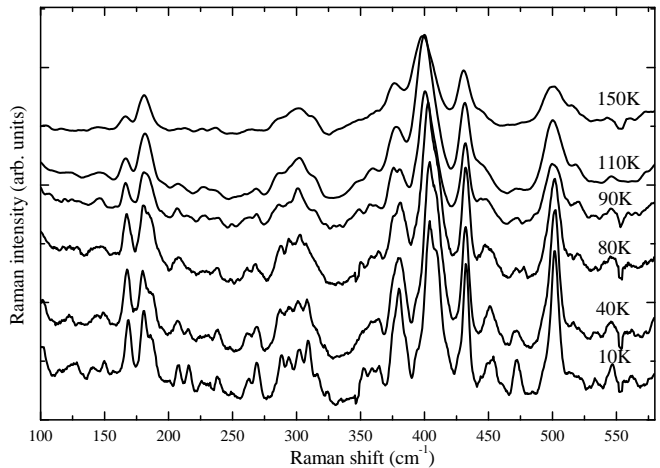


FIG. 4: Temperature dependence of the Raman spectra from 10 K to 150 K in parallel polarization configuration. No difference in number of phonon modes is observed.

Figure 3 shows low temperature Raman spectra obtained at 10 K. We have reported the frequencies of the A_g and E_g modes in Table I. Our results are compared to the measurements of Ref. 20. We have been able to identify 37 modes compared to Ref. 20. Notice that it was not possible with the Raman selection rules to determine the symmetry of low intensity peaks. It is clearly visible that more than 12 Raman modes are observed. Although this large number of modes could be explained by a low quality of the single-crystal samples, we discarded that possibility due to several characterizations (X-ray and neutron diffraction) that have demonstrated their quality. Moreover, there is no evidence of nano-domains in the characterization measurements^{11,12,23}. Additionally, the modes observed in the Raman spectra seem too sharp and their energies are too low to be due to second order processes. One can also notice that the Raman spectra shown in Iliev et al.²⁰ exhibit an equivalent number of modes for crystals from a different source.

To study the coupling between the lattice and the magnetic orders, we measured the temperature dependences of the phonon modes. Figure 4 presents the Raman spectra from 4 K to 150 K above 100 cm^{-1} . We can observe that the number of phonon modes seems to increase around the magnetic transitions at 90 K and 50 K. It has been shown by Slawinski et al.²¹ that the magnetic transitions are associated to incommensurate modulation of the atomic positions. All phonon modes might become both Raman and infrared active due to the modulation and in particular out-of-center phonon modes might become Raman active and visible in our spectra. Part of the additional modes might be related to the symmetry rule breaking due to the incommensurate transition but it might be also necessary to consider a new space group for the structure at low temperatures.

Figure 5 shows the behavior in temperature of three phonon modes: the A_g mode at 432 cm^{-1} and the two E_g

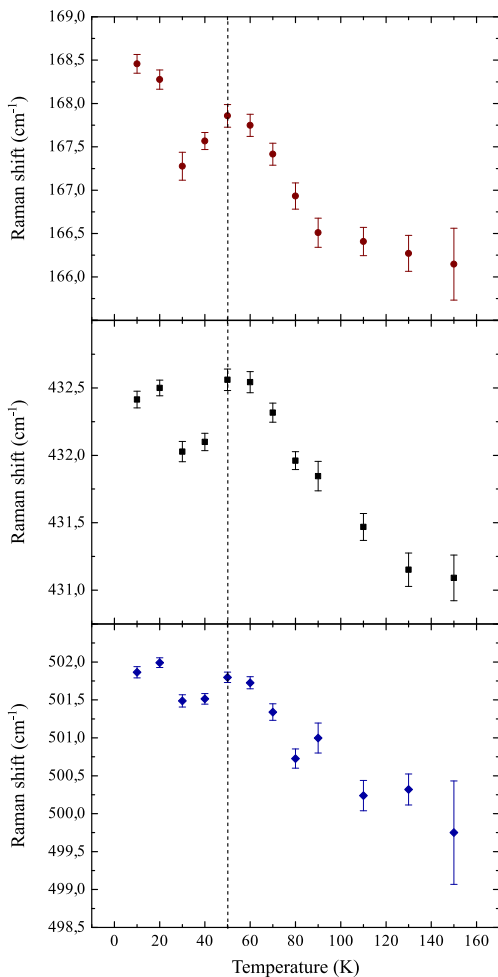


FIG. 5: Temperature dependence of 168.5, 432.5 and 502 cm^{-1} phonon modes's wavenumber. The dotted line correspond to the T_{N2} magnetic transition temperature.

modes at 168 and 502 cm^{-1} . All the phonon frequencies soften due to the dilation of the unit cell when temperature increases. These phonon modes present an abrupt change in their frequencies around the lowest magnetic transition temperature $T_{N2} \simeq 50$ K that can be interpreted as the fingerprint of a spin-phonon coupling at this magnetically-ordered phase. We can notice that the first magnetic transition at 90 K can induce changes in the Raman mode frequencies due to the direct coupling between the magnetic ordering and lattice since there is no anomaly in the lattice parameters at this magnetic transition. No significant changes in the mode frequencies has been measured at this transition. However, at the second magnetic transition the lattice parameters change significantly and the spin-phonon coupling anomalies we are measuring at 50 K could be due to the magnetostriction effect evidenced by Nonato *et al.*²². The Ag mode at 432 cm^{-1} has been associated to Mn(B)O₆ (B position of the perovskite) rotations around the [111] cubic diagonal.²⁰ This mode is quite important because it is

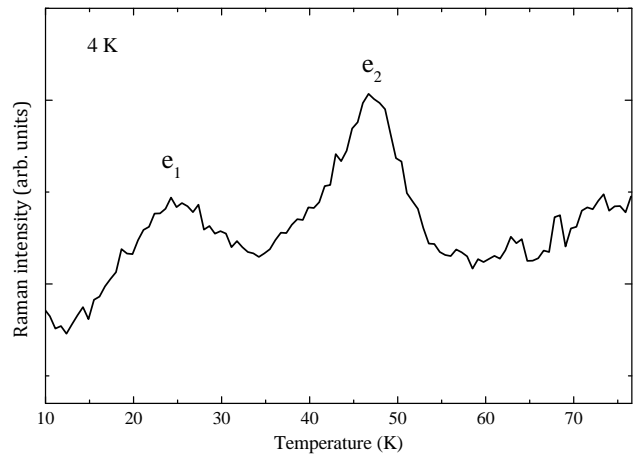


FIG. 6: Low energy Raman excitations measured at 4 K in $\text{CaMn}_7\text{O}_{12}$ in parallel polarization configuration.

the only Ag mode to survive at high temperatures in the Im $\bar{3}$ phase with disordered Jahn-Teller distortions.²⁰ The abrupt change of slope at 50 K shows that the new modulation of the Mn spin in the (a,b) plane, possibly driven by the magnetostriction effect, controls this mode. Notice that Nonato *et al.*²² have observed anomalies in the phonon frequencies in polycrystalline compounds. They observed an inversion of the frequency slope around 50 K for a peak at 378.8 cm^{-1} (376 cm^{-1} in our measurements). We have also detected a shift but within our experimental error bars. We have not detected the strong shift detected for the 625 cm^{-1} peak around 60 K and 90 K. Such a discrepancy might originate from the samples (monocrystal versus polycrystal).

B. Low energy excitations

Figure 6 shows the low energy Raman spectrum obtained at 4 K in parallel polarization configuration. Two large low-energy Raman excitations labeled e_1 and e_2 are visible around 25 and 47 cm^{-1} , respectively.

To have a better insight on the nature of these two excitations, the temperature dependence of the low energy Raman spectra have been recorded between 4 K and 150 K in Fig. 7(a).

In Fig. 7(b), the e_1 lower energy excitation disappears at the magnetic transition ($T_{N1} \simeq 50$ K) whereas the e_2 excitation at 47 cm^{-1} survives above this temperature to disappear at the magnetic transition $T_{N2} \simeq 90$ K. The e_1 excitation is thus connected to the modulation of the magnetic order occurring in the AFM_{II} state and e_2 excitation is related to the AFM_I ordering of the Mn spins in the (a, b) planes with spiral propagation along the 3-fold axis. Remember that this transition is reportedly responsible for the appearance of the ferroelectric order. Notice that the frequency of the e_2 excitation downshifts below the second magnetic phase. This behavior indicates

a sensitivity of this excitation to the magnetic modulation occurring at 50 K. Our observations are in agreement with the measures published by Kadlec et al.²⁴ where they measured using Infrared spectroscopy electromagnons excitations at the same energies. On the contrary, these modes don't remain active in the paramagnetic phase and we have not observed paraelectromagnons. A soft mode has also been reported at around 80cm⁻¹ at low temperatures (10 K)^{18,19}. Although we didnt report this mode in our study, the signal over noise ratio of our low energy Raman data is not allowing us to exclude with certainty the observation of this mode.

IV. CONCLUSION

In summary, the high number of phonon modes observed in CaMn₇O₁₂ rises the question of the space group of this compound at low temperature. The temperature dependance of the lattice excitations in CaMn₇O₁₂ show the role plays by magnetostriction coupling in this compound. In particular, the Ag mode at 432 cm⁻¹ associated to Mn(B)O₆ rotations around the [111] cubic diagonal is modified the modulation of the Mn spin in the (a,b) at 50 K. We were able to measure low energy Raman excitations in CaMn₇O₁₂ and observed two large excitations around 25 and 47 cm⁻¹. We show that they are linked to the two different magnetic orderings occurring below 90 and 50 K and are interpreted as the Raman signature of CaMn₇O₁₂'s electromagnons.

Acknowledgments

This work was supported in part by the French National Research Agency (ANR) through DYMMOS

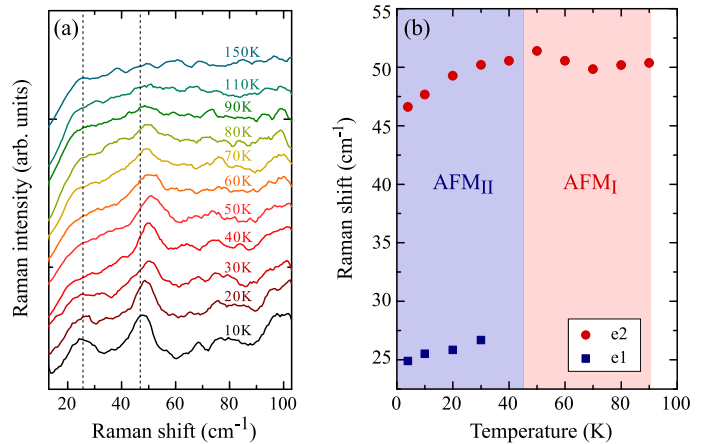


FIG. 7: Temperature dependence of : (a) low energy Raman spectra of CaMn₇O₁₂ between 10 and 150 K, (b) the Raman shift of the e₁ (square) and e₂ (circle) low energy excitations as a function of the temperature.

project and by the General Directorate for Armament (DGA).

* Present address : Materials for Research and Technology - Ferroic Materials for Transducers, Luxembourg Institute of Science and Technology, 41 rue du Brill, L-4422 Belvaux, Luxembourg; Corresponding Author : constance.toulouse@list.lu
 † Present address : Institut Néel, CNRS/UGA UPR2940, 25 rue des Martyrs BP 166, 38042 Grenoble cedex 9
¹ W. Eerenstein, D. D. Mathur, and J. F. Scott, *Nature* **442**, 759 (2006).
² T. Zhao *et al.*, *Nature Materials* **5**, 823 (2006).
³ D. Senff, P. Link, K. Hradil, A. Hiess, L. P. Regnault, Y. Sidis, N. Aliouane, D. N. Argyriou, and M. Braden, *Phys. Rev. Lett.* **98**, 137206 (2007).
⁴ D. Khomskii, *Physics* **2**, 20 (2009).
⁵ J. Wang *et al.*, *Science* **299**, 1719 (2003).
⁶ S. W. Cheong and M. Mostovoy, *Nature Mater.* **6**, 13 (2007).
⁷ I. A. Sergienko and E. Dagotto, *Phys. Rev. B* **73**, 094434 (2006).
⁸ R. E. Newnham, J. J. Kramer, W. A. Schulze, and L. E. Cross, *J. Appl. Phys.* **49**, 6088 (1978).
⁹ J. Blasco, C. Ritter, J. Garcia, J. M. de Teresa, J. Perez-Cacho, and M. R. Ibarra, *Phys. Rev. B* **62**, 5609 (2000).
¹⁰ G. Zhang, S. Dong, Z. Yan, Y. Guo, Q. Zhang, S. Yunoki, E. Dagotto, and J.-M. Liu, *Phys. Rev. B* **84**, 174413 (2011).
¹¹ R. D. Johnson, L. C. Chapon, D. D. Khalyavin, P. Manuel, P. G. Radaelli, and C. Martin, *Phys. Rev. Lett.* **108**, 067201

(2012).
¹² N. J. Perks, R. D. Johnson, C. Martin, L. C. Chapon, and P. G. Radaelli, *Nat. Comm.*, **3**, 1277 (2012).
¹³ X. Z. Lu, M. H. Whangbo, S. Dong, X. G. Gong, and H. J. Xiang, *Phys. Rev. B* **108**, 187204 (2012).
¹⁴ N. Terada, Y. S. Glazkova, and A. A. Belik, *Phys. Rev. B* **93**, 155127 (2016).
¹⁵ R. Przenioslo, I. Sosnowska, E. Suard, A. Hewat, and A. N. Fitch, A. N., *J. Phys.: Cond. Mat.* **14**, 5747 (2002).
¹⁶ J. S. Lim, D. Saldana-Greco, and A. M. Rappe, *Phys. Rev. B* **97**, 045115 (2018).
¹⁷ M. Sánchez-Andújar, S. Yáñez-Vilar, N. Biskup, S. Castro-García, J. Mira, J. Rivas, and M. A. Señarís-Rodríguez, *J. Magn. Magn. Mater.* **321**, 1739 (2009).
¹⁸ X. Du, R. Yuan, L. Duan, C. Wang, Y. Hu, and Y. Li, *Phys. Rev. B* **90**, 104414 (2014).
¹⁹ S. M. Souliou, Y. Li, X. Du, M. Le Tacon, and A. Bosak, *Phys. Rev. B* **94**, 184309 (2016).
²⁰ M. N. Iliev, V. G. Hadjiev, M. M. Gospodinov, R. P. Nikolova, and M. V. Abrashev, *Phys. Rev. B* **89**, 214302 (2014).
²¹ W. Ślawinski, R. Przenioslo, I. Sosnowska, A. and A. Chrobak, *J. Phys. Soc. Jpn* **81**, 094708 (2012).
²² A. Nonato, B. S. Araujo, A. P. Ayala, A. P. Maciel, S. Yanez-Vilar, M. Sanchez-Andujar, M. A. Senaris-Rodriguez, and C. W. A. Paschoal, *Appl. Phys. Lett.* **105**, 222902 (2014).

- ²³ R. D. Johnson, D. D. Khalyavin, P. Manuel, A. Bombardi, C. Martin, L. C. Chapon, and P. G. Radaelli, *Phys. Rev. B* **93**, 180403(R) (2016).
- ²⁴ F. Kadlec, V. Goian, C. Kadlec, M. Kempa, P. Vanek, J.

Taylor, S. Rols, J. Prokleška, M. Orlita, and S. Kamba, *Phys. Rev. B* **90**, 054307 (2014).